2007 Jan; 71(1): 89-94
14) Takaki A, Ogawa H, Wakeyama T, Iwami T, Kimura M, Hadano Y, Matsuda S, Miyazaki Y, Matsuda T, Hiratsuka A, Matsuzaki M: Cardio-ankle vascular index is a new noninvasive parameter of arterial stiffness. Circ J, 2007 Nov; 71(11): 1710-1714
15) Ibata J, Sasaki H, Kakimoto T, Matsuno S, Nakatani M, Kobayashi M, Tatsumi K, Nakano Y, Wakasaki H, Furuta H, Nishi M, Nanjo K: Cardio-ankle vascular index measures arterial wall stiffness independent of blood pressure. Diabetes Res Clin Pract, 2008; 80(2): 265-270
16) Okura T, Watanabe S, Kurata M, Manabe S, Koresawa M, Irita J, Enomoto D, Miyoshi K, Fukuoka T, Higaki J: Relationship between cardio-ankle vascular index (CAVI) and carotid atherosclerosis in patients with essential hypertension. Hypertens Res, 2007 Apr; 30(4): 335-340
17) Nakamura K, Tomaru T, Yamamura S, Miyashita Y, Shirai K, Noike H: Cardio-ankle vascular index is a candidate predictor of coronary atherosclerosis. Circ J, 2008 Apr; 72(4): 598-604
18) Ichihara A, Yamashita N, Takemitsu T, Kaneshiro Y, Sakoda M, Kurauchi-Mito A, Itoh H: Cardio-ankle vascular index and ankle pulse wave velocity as a marker of arterial fibrosis in kidney failure treated by hemodialysis. Am J Kidney Dis, 2008 Nov; 52(5): 947-955
19) Nakamura K, Takuo Iiduka, Mao Takahashi, Kazuhiro Shimizu, Hiroshi Mikamo, Takahiro Nakagami, Masayo Suzuki, Keiichi Hirano, Yuko Sugiyama, Takanobu Tomaru, Yoh Miyashita, Kohji Shirai, and Hirofumi Noike: Association between Cardio-Ankle Vascular Index and Serum Cystain C Levels in Patients with Cardiovascular Risk Factor. J Atheroscler Thromb, 2009; 16(4): 371-379
20) Hayashi G, Sato M, Niimi H, Handa H, Moritake K, Okumura: Analysis of vascular wall constitutive law with finite deformation theory. Medical Electronics and Biological Engineering, 1975; 13; 293-297
21) Kawasaki T, Sasayama S, Yagi S: Noninvasive assessment of the age related changes in stiffness of major branches of the human arteries. Cardiovascular Res, 1987; 21: 678-687
22) Stenberg J, Wasir H, Amery A, Sannerstedt R, Werko L; Comparative hemodynamic studies in man of adrenergic beta1 receptor blocking agents without or with intrinsic sympathomimetic activity. Acta Pharmacol Toxicol, 1975; 36(supple. V):70-76
23) Regårdh CG, Borg KO, Johansson R, Johnson G, Palmer L: Pharmacokinetic studies on the selective beta1-receptor antagonist metoprolol in man. J Pharmacokinet Biopharm, 1974; 2(4): 347-364
24) Alabaster VA, Davey MJ: The alpha 1-adrenoceptor antagonist profile of doxazosin: preclinical pharmacology. Br J Clin Pharmacol, 1986; 21 Suppl 1: 9S-17S
25) Vincent J, Elliott HL, Meredith PA, Reid JL: Doxazosin, an alpha 1-adrenoceptor antagonist: pharmacokinetics and concentration-effect relationships in man. J Clin Pharmacol, 1983; 15(6): 719-725
26) Murata K, Motayama T, Kotake C: Collagen types in various layers of the human aortaand their changes with atherosclerotic process. Atherosclerosis, 1986; 60(3): 251-262
27) Papakonstantinou E, Roth M, Block LH, Mirtsou-Fidani V, Argiriadis P, Karakiulakis G: The differential distribution of hyaluronic acid in the layers of human atheromatic aortas is associated with vascular smooth muscle cell proliferation and migration. Atherosclerosis 1998; 138: 79-89
28) Ross R; The pathogenesis of atherosclerosis: a perspective for the 1990s. Nature, 1993; 29; 362(6423): 801-809
29) Metaka F, Niu H: Biophysical Effects of Adrenaline on the Smooth Muscle of the Rabbit Common Carotid Artery. J Gen Physiol, 1972; 59: 92-I02 2
30) Dzau VJ, Re R: Tissue angiotensin system in cardiovascular medicine. A paradigm shift? Circulation, 1994; 89(1): 493-498
31) Lam YW, Giard MJ, Warren JB: Calcium channel blockers and treatment of hypertension. Drug Intell Clin Pharm, 1986; 20(3): 187-198
32) Palmer RM, Ferrige AG, Moncada S: Nitric oxide release accounts for the biological activity of endothelium-derived relaxing factor. Nature, 1987; 327(6122): 524-526
33) Su, MD Kun-Tai Lee, Chih-Sheng Chu Ming-Yi Lee, Tsung-Hsien Lin Wen-Chol Voon, Sheng-Hsiung Sheu, Wen-Ter Lai: Effects of Heart Rate on Brachial-Ankle Pulse Wave Velocity and Ankle-Brachial Pressure Index in Patients Without Significant Organic Heart Disease. Angiology, 2007; 58(1): 67-74

Int J Hematol (2010) 91:611–619
DOI 10.1007/s12185-010-0563-3

ORIGINAL ARTICLE

Depletion of Dnmt1-associated protein 1 triggers DNA damage and compromises the proliferative capacity of hematopoietic stem cells

Tomoe Koizumi · Masamitsu Negishi · Shunsuke Nakamura · Hideyuki Oguro · Kaneshige Satoh · Masaharu Ichinose · Atsushi Iwama

Received: 21 September 2009 / Revised: 17 March 2010 / Accepted: 17 March 2010 / Published online: 14 April 2010

Abstract Dnmt1-associated protein 1 (Dmap1) is a core component of the NuA4 histone acetyltransferase complex and the Swr1 chromatin-remodeling complex. However, the cellular function of Dmap1 remains largely unknown. We previously reported that Dmap1 plays a crucial role in DNA repair and is indispensable for the maintenance of chromosomal integrity of mouse embryonic fibroblasts. In this study, we examined the role of Dmap1 in self-renewing HSCs. *Dmap1*-knockdown induced by *Dmap1*-specific shRNA severely compromised the proliferative capacity of HSCs in vitro and long-term repopulating capacity of HSCs in recipient mice. *Dmap1*-knockdown in HSCs triggered DNA damage as evident by the formation of foci of γ-H2AX and activated p53-dependent cell cycle checkpoints. Deletion of *p53* in HSCs abrogated the activation of p53-dependent cell cycle checkpoints, but did not restore the HSC function impaired by the knockdown of *Dmap1*. These findings suggest that Dmap1 is essential for the maintenance of genomic integrity of self-renewing HSCs and highlight DNA damage as one of the major stresses causing HSC depletion.

T. Koizumi · M. Negishi · S. Nakamura · H. Oguro · A. Iwama (✉)
Department of Cellular and Molecular Medicine, Graduate School of Medicine, Chiba University, 1-8-1 Inohana, Chuo-ku, Chiba 260-8670, Japan
e-mail: aiwama@faculty.chiba-u.jp

T. Koizumi · K. Satoh · M. Ichinose
Department of Plastic Surgery, Graduate School of Medicine, Chiba University, Chiba 260-8670, Japan

M. Negishi · S. Nakamura · H. Oguro · A. Iwama
JST, CREST, Sanbancho, Chiyoda-ku, Tokyo 102-0075, Japan

Keywords Dnmt1-associated protein 1 (Dmap1) · DNA repair · Hematopoietic stem cells (HSCs) · Genomic integrity

1 Introduction

Chromatin modifications can occur through epigenetic mechanisms, including histone post-translational modifications by chromatin-modifying enzymes and chromatin structural modifications by ATP-dependent chromatin-remodeling complexes. Chromatin modifications play a critical role in regulating the balance between multipotency and differentiation of stem cells by promoting changes in the nucleosomal organization [1–3]. Dnmt1-associated protein 1 (DMAP1) was originally reported to interact with DNMT1 and to co-localize with PCNA and DNMT1 at the DNA replication foci during the S phase in human cells [4]. Recent studies have revealed that DMAP1 is a core component of the NuA4/Tip60 histone acetyltransferase (HAT) complex and the ATP-dependent chromatin-remodeling complex Swr1 in yeast or Snf2-related CREB-binding protein activator protein (SRCAP) in human [5]. These complexes are conserved from yeast to mammals and function in DNA replication, repair and homologous recombination [6].

DMAP1 and a SWI2/SNF2 family ATPase, p400/Domino, are two core components of the NuA4/Tip60 complex and contain a highly conserved SANT (SWI3-ADA2-NcoR-TFIIIB) domain, a histone tail-binding module [7]. Both subunits are critical to yeast cell viability and function in cell cycle progression and transcriptional regulation [8]. Deletion mutants of their yeast homologs are highly sensitive to DNA breaks induced by DNA-damaging agents, such as hydroxyurea and methyl

methanesulfonate (MMS), suggesting an essential role for these two proteins in cell cycle progression, transcriptional regulation and DNA repair [9]. However, the role of DMAP1 in mammalian cells has not been elucidated.

We previously reported that Dmap1 interacts with the polycomb group protein Bmi1, an essential regulator of hematopoietic stem cells (HSCs) [10–12], and is involved in Bmi1-mediated transcriptional repression at some loci at least [13]. We further reported that Dmap1 interacts with proliferating cell nuclear antigen (PCNA) during DNA damage and that reduced expression of Dmap1 in mouse embryonic fibroblasts (MEFs) causes spontaneous DNA breaks and genomic instability due to inhibition of PCNA accumulation at the damaged sites [14]. These findings suggest that Dmap1 plays crucial roles in the repair of damaged DNA in mammals. Recently, DNA damage appeared to be intimately linked to stem cell aging, causing HSC depletion over time [15–17].

Based on these findings, we performed lentiviral-mediated RNA interference of *Dmap1* in HSCs to better understand the role of Dmap1 in HSCs. We show that depletion of Dmap1 triggers DNA damage and compromises the proliferative capacity of HSCs. Our findings indicate that Dmap1 is involved in mammalian DNA repair and plays an essential role in the maintenance of HSCs.

2 Materials and methods

2.1 Mice

C57BL/6 (B6-Ly5.2) mice were purchased from Japan SLC (Shizuoka, Japan). C57BL/6 mice congenic for the Ly5 locus (B6-Ly5.1) were purchased from Sankyo-Lab Service (Tsukuba, Japan). $p53^{+/-}$ mice (Acc. No. CDB0001K) that had been backcrossed at least eight times onto a C57BL/6 (B6-Ly5.2) background were obtained from RIKEN BRC (Tsukuba, Japan). Mice were bred and maintained in the Animal Research Facility of the Graduate School of Medicine, Chiba University in accordance with our institutional guidelines.

2.2 Purification of mouse HSCs

Mouse HSCs ($CD34^-KSL$ cells) [18] were purified from bone marrow (BM) cells of 8-week-old mice. In brief, low-density cells were isolated on Ficoll-Paque™ PLUS (GE Healthcare, Uppsala, Sweden). The cells were stained with an antibody cocktail consisting of biotinylated anti-Gr-1, Mac-1, B220, CD4, CD8 and Ter-119 monoclonal antibodies (PharMingen, San Diego, CA). Lineage-positive cells were immunomagnetically enriched using anti-rat IgG microbeads (Miltenyi Biotech, Auburn, CA). The cells were further stained with fluorescein isothiocyanate (FITC)-conjugated anti-CD34, phycoerythrin (PE)-conjugated anti-Sca-1 and allophycocyanin (APC)-conjugated anti-c-Kit antibodies (PharMingen). Biotinylated antibodies were detected with streptavidin-APC-Cy7 (PharMingen). Four-color analysis and sorting were performed on a JSAN cell sorter (Bay Bioscience, Kobe, Japan).

2.3 *Dmap1*-knockdown and transduction of $CD34^-KSL$ cells

Lentiviral vectors (CS-H1-shRNA-EF-1α-EGFP) expressing shRNA against murine *Dmap1* (target sequence: #1 GGCACAGATCTCAAGATAC, and #2 GTGCCAACTG TGAATATGA) and *luciferase* were prepared and the viruses were produced as described [14]. Briefly, plasmid DNA was transfected into 293T cells along with the packaging plasmid (pCAG-HIVgp) and the VSV-G- and Rev-expressing plasmid (pCMV-VSV-G-RSV-Rev) by $CaPO_4$ coprecipitation. Supernatants from transfected cells were concentrated by centrifugation at 6,000*g* for 16 h, and then resuspended in α-MEM supplemented with 1% FCS (1/100 of the initial volume of supernatant). Viral titers were determined by infection of Jurkat cells (a human T-cell line). $CD34^-KSL$ cells were deposited into recombinant fibronectin fragment (Takara Shuzo, Otsu, Japan)-coated 96-well micro-titer plates, at 100–150 cells per well, and incubated in α-MEM supplemented with 1% FBS, 100 ng/ml mouse stem cell factor (SCF) and 100 ng/ml human thrombopoietin (TPO) (Peprotech, Rocky Hill, NJ) for 24 h. Then, cells were transduced with a lentivirus vector at a multiplicity of infection (MOI) of 1,000 in the presence of protamine sulfate (5 μg/ml; Sigma, St. Louis, MO) for 24 h. After transduction, cells were further incubated in S-Clone SF-O3 (Sanko Junyaku, Tokyo, Japan) supplemented with 1% FBS, 100 ng/ml SCF and 100 ng/ml TPO for 12 h and subjected to an in vitro colony assay or liquid culture, or incubated in S-Clone SF-O3 supplemented with 0.1% BSA (Sanko Junyaku), 100 ng/ml SCF and 100 ng/ml TPO for 36 h and subjected to a competitive repopulation assay. The transduction efficiency was >90% in most experiments as judged from the GFP expression observed under an inverted microscope.

2.4 Colony assay

$CD34^-KSL$ cells transduced with indicated lentiviruses were plated in methylcellulose medium (Stem Cell Technologies, Vancouver, BC) supplemented with 20 ng/ml mouse SCF, 20 ng/ml mouse IL-3 (Peprotech), 50 ng/ml human TPO and 2 units/ml human erythropoietin (EPO) (Peprotech). The culture dishes were incubated at 37°C in a 5% CO_2 atmosphere. GFP^+ colony numbers were counted

on day 14. Colonies were recovered, cytospun onto glass slides and then subjected to May-Grüenwald Giemsa staining for morphological examination.

2.5 Competitive repopulation assay

Fifty HSCs from B6-ly5.2 mice transduced with knockdown viruses against *Dmap1* or *luciferase* were mixed with 2×10^5 BM competitor cells (B6-Ly5.1) and transplanted into B6-Ly5.1 mice irradiated with a dose of 9.5 Gy. Donor cell chimerism in the recipient peripheral blood cells was evaluated as described previously [18].

2.6 Semiquantitative RT-PCR

Semi-quantitative RT-PCR was carried out using normalized cDNA with TaqMan rodent GAPDH control reagent (Perkin-Elmer Applied Biosystem, Foster City, CA). Primer sequences and amplification conditions are available from the authors on request.

2.7 Immunofluorescent analysis

HSCs that had been infected with the knockdown virus were fixed with 3% formaldehyde or 1.5% paraformaldehyde in PBS for 10 min at room temperature, washed and treated with 0.2% Triton X-100 in PBS for 5 min. After blocking with 10% goat serum for 60 min, the coverslips were incubated with an anti-H2AX-pS139 antibody (Cell Signaling Technology, Danvers, MA) for 60 min at room temperature, and then washed and incubated with Alexa 555 anti-rabbit IgG (Invitrogen, Carlsbad, CA) for 60 min at room temperature. The percentage of γ-H2AX foci per cell was determined by examining more than 50 cells per glass slide. Images were taken with a Nikon eclipse 80i fluorescence microscope and processed using Adobe PhotoShop CS3 (Adobe Systems Inc., San Jose, CA). Apoptosis was evaluated by immunostaining using an anti-active caspase-3 antibody (Cell Signaling Technology).

2.8 Cell culture and proliferation assay

NIH3T3 cells were maintained in Dulbecco's modified Eagle's medium supplemented with 10% fetal bovine serum and 1% penicillin–streptomycin at 37°C under 10% CO_2 in a humidified incubator. For the cell proliferation assay, cells were infected with lentiviruses expressing shRNA against either *luciferase* or *Dmap1*. At 48 h after infection, 5×10^4 cells were spread into 12-well plates and cultured. Cell numbers were counted each day for six consecutive days.

2.9 Senescence-associated-β-galactosidase assay

Senescence-associated-β-galactosidase activity was determined using an SA-β-gal staining kit from Cell Signaling Technology (Beverly, MA) according to the manufacturer's instruction. Senescent cells were identified as blue-stained cells under an inverted microscope.

3 Results

3.1 *Dmap1*-knockdown compromises the proliferation of HSCs

To evaluate the cellular function of Dmap1 in HSCs, we first examined the expression profile of *Dmap1* in various BM hematopoietic cell fractions by semi-quantitative RT-PCR. *Dmap1* was detected in all fractions, but at higher levels in lineage marker-negative (Lin^-) cells and $CD34^-$ c-Kit^+Sca-1^+Lineage $marker^-$ stem cells ($CD34^-$KSL) HSCs (Fig. 1a).

To explore the contribution of Dmap1 to the proliferation and differentiation of HSCs, we purified the $CD34^-$KSL HSC fraction in murine BM cells, which is highly enriched for long-term repopulating HSCs [18], and knocked down *Dmap1* by infecting the HSCs with a lentivirus expressing *Dmap1*-specific shRNA (shRNA1 and 2) [14]. We first evaluated the mRNA expression levels of *Dmap1* and the cell proliferation of murine fibroblast NIH3T3 cells expressing *Dmap1* shRNA (shRNA1 or 2). *Dmap1*-knockdown using shRNAs (shRNA1 or 2) showed significantly reduced expression of *Dmap1* mRNA in RT-PCR analysis compared to those in control cells infected with shRNA against *luciferase* (*Luc*-KD) (Fig. 1b). We used *Dmap1*-shRNA1 (*Dmap1*-KD) in the subsequent experiments and monitored GFP expression to evaluate the infection efficacy in each experiment. Interestingly, *Dmap1*-knockdown in NIH3T3 cells caused mild growth retardation (Fig. 1c).

Of note, HSCs infected with shRNA against *Dmap1* showed marked growth retardation (Fig. 2a, left panel). The percentage of GFP^+-infected cells progressively decreased in the *Dmap1*-knockdown culture while it stayed at a high level in the control *Luciferase*-knockdown culture (Fig. 2a, middle panel), demonstrating severely suppressed cell growth of GFP^+ *Dmap1*-knockdown cells (Fig. 2a, right panel). *Dmap1* shRNA2 also had a very similar effect to that of shRNA1 on the growth of HSCs, although the transduction efficiency was not high in these experiments (Fig. 2b). We next examined the colony-forming capacity of *Dmap1*-knockdown HSCs. The knockdown significantly decreased the total number of colony-forming cells (CFCs), particularly that of high proliferative potential

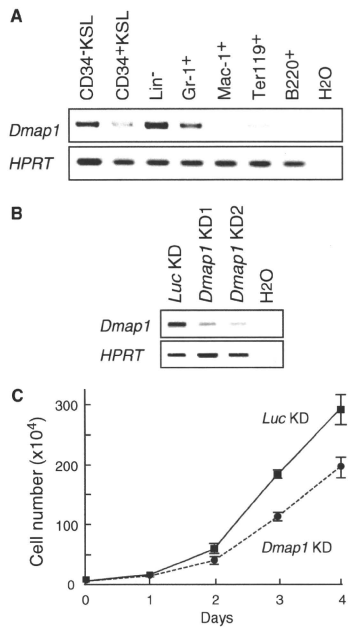

Fig. 1 Expression of *Dmap1* in hematopoietic cells. **a** mRNA levels of mouse *Dmap1* in hematopoietic cells. Cells analyzed are BM $CD34^-$c-$Kit^+Sca\text{-}1^+$Lineage marker$^-$ stem cells ($CD34^-KSL$), $CD34^+KSL$ progenitors, Lineage marker$^-$ cells (Lin^-), $Gr\text{-}1^+$ neutrophils, $Mac\text{-}1^+$ monocytes/macrophages, $Ter119^+$ erythroblasts, and $B220^+$ B cells. **b** The levels of *Dmap1* mRNA in *Dmap1*-KD NIH3T3 cells. Hypoxanthine guanine phosphoribosyl transferase (*HPRT*) was used as a control. **c** Growth curve of NIH3T3 cells expressing *Luciferase* or *Dmap1*-specific shRNA. Data are presented as the mean ± SD for triplicate cultures

colony-forming cells (HPP-CFCs; colony diameter >1 mm) rather than low proliferative potential CFCs (LPP-CFCs; colony diameter <1 mm) (Fig. 2c). Morphological characterization of colonies revealed that *Dmap1*-depleted HSCs retained multi-lineage differentiation potential and gave rise to colonies consisting of multi-lineage cells represented by neutrophil/macrophage/erythroblast/megakaryocyte (nmEM) colonies (Fig. 2d).

3.2 *Dmap1*-knockdown compromises the repopulating capacity of HSCs

To examine the effect of *Dmap1*-knockdown in vivo, we performed a competitive repopulation assay. As expected from the in vitro proliferation assay data, *Dmap1*-knockdown HSCs showed a severely impaired repopulation capacity, both short-term and long-term (Fig. 3a). The total chimerism of CD45.1 donor cells in peripheral blood was low and that of the GFP^+ transduced cells expressing shRNA against *Dmap1* was even lower (Fig. 3b). As in vitro, however, *Dmap1*-knockdown HSCs showed multi-lineage differentiation including T- and B-cell lineages in vivo (Fig. 3b).

3.3 *Dmap1*-knockdown activates a p53-dependent checkpoint and causes DNA damage in HSCs

To understand how *Dmap1*-knockdown in HSCs led to growth suppression, we examined the transcriptional regulation in *Dmap1*-depleted cells. We found that depletion of Dmap1 led to increased expression of some of the p53 downstream targets, $p21^{Cip1/Waf1}$, *Noxa*, *Puma* and *Bax* (Fig. 4a). The NuA4 HAT complex functions as a cofactor of p53-dependent transcriptional regulation [19]. p53 is a key component of damage-response signaling pathways, serving to activate checkpoints [20]. Therefore, we purified HSCs from $p53^{-/-}$ mice and examined the transcriptional levels of p53 target genes in *Dmap1*-depleted HSCs by RT-PCR. Transcriptional up-regulation of p53 target genes, including $p21^{Cip1/Waf1}$, *Noxa*, *Puma* and *Bax* by *Dmap1*-knockdown was canceled in a *p53*-deficient background (Fig. 4b). These expression profiles suggest that *p53*-dependent checkpoint is activated by *Dmap1*-knockdown in HSCs at least to a certain extent.

One of the p53 target genes, $p21^{Cip1/Waf1}$, plays a pivotal role in the determination of cell fate, apoptosis or cellular senescence, when cells are exposed to cytotoxic stress. Although the expression of pro-apoptotic p53 target genes, *Puma* and *Noxa*, was highly up-regulated in *Dmap1*-depleted HSCs, less apoptotic cell death was detected by caspase-3 staining (Fig. 4c). Nonetheless, stress-induced cellular senescence was not evident in *Dmap1*-knockdown HSCs, as judged by SA-β-galactosidase staining (Fig. 4d).

The NuA4 HAT multi-subunit complex is responsible for the acetylation of histone H4 and H2A N-terminal tails and for the incorporation of the variant H2A.Z in chromatin, both of which are critical for the normal repair of double-strand breaks, including homologous recombination [8]. We recently reported that Dmap1 interacts with PCNA during DNA damage, and *Dmap1*-knockdown in MEFs causes spontaneous DNA breaks and genomic instability [14]. These findings suggest that Dmap1 plays crucial roles in the repair of damaged DNA in mammals. Therefore, we determined the phosphorylation status of H2AX at Ser139 (γ-H2AX), a marker of DNA breaks [21], to test whether the knockdown of *Dmap1* also causes

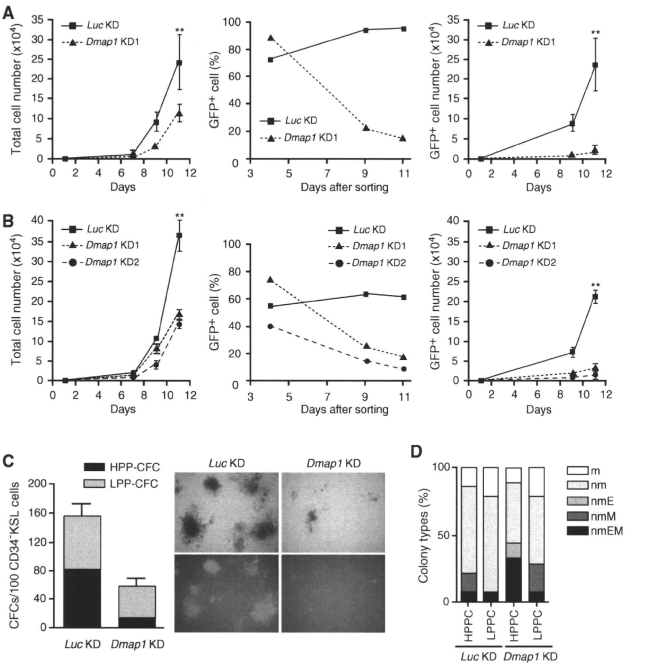

Fig. 2 *Dmap1*-knockdown compromises the proliferation of HSCs. **a**, **b** Growth of *Luc*-KD or *Dmap1*-KD CD34$^-$KSL HSCs in vitro. The effect of *Dmap1* KD1 shRNA was evaluated in **a** and effects of *Dmap1* KD1 and 2 shRNAs were compared in **b**. Total cell numbers were plotted (*left panel*). The results are shown as the mean ± SD for triplicate cultures. Proportion of GFP-positive cells in *Luc*-KD or *Dmap1*-KD HSC cultures were determined by flow cytometric analysis on the indicated days (*middle panel*) and the absolute numbers of GFP$^+$ cells were plotted (*right panel*), $^{**}p < 0.05$. **c** Colony assay of *Luc*-KD or *Dmap1*-KD CD34$^-$KSL HSCs. CD34$^-$KSL cells were transduced with *Luc*-KD or *Dmap1*-KD, and at 36 h after the initiation of transduction, plated in methylcellulose medium in the presence of SCF, IL-3, TPO, and EPO to allow colonies to form. The numbers of high and low proliferative potential colony-forming cells (HPP-CFC and LPP-CFC) were retrospectively evaluated by counting colonies at day 14 (HPP-CFC and LPP-CFC: colony diameter >1 and <1 mm, respectively) (*left panel*). The results are shown as the mean ± SD for triplicate cultures. Photomicrographs of representative colonies observed under an inverted microscope at a magnification of ×40 are depicted (*right upper panel* bright field, *right lower panel* fluorescent field). The transduction efficiency was over 90% as in **a** as judged from the GFP expression observed under an inverted microscope. **d** Frequency of each colony type. Colonies derived from *Luc*-KD or *Dmap1*-KD HPP-CFC or LPP-CFC were recovered and the composition of colony-forming cells was examined morphologically. The following abbreviations were used: *n* neutrophil, *m* macrophage, *E* erythroblast, *M* megakaryocyte

spontaneous DNA damages in HSCs. HSCs were infected with lentivirus encoding *Dmap1* or *Luciferase* shRNA, and were subjected to immunofluorescent analysis of γ-H2AX after 72 h of infection. *Dmap1*-knockdown HSCs showed a significantly increased number of foci of γ-H2AX compared to the control HSCs (Fig. 5). These results indicate that depletion of Dmap1 caused spontaneous DNA breaks in HSCs.

3.4 *Dmap1*-knockdown HSCs show robust growth suppression even with disruption of p53-dependent checkpoints

To examine the effect of the activation of p53-dependent checkpoints on growth suppression in *Dmap1*-depleted HSCs, we knocked down *Dmap1* in *p53*$^{-/-}$ HSCs to cancel p53-dependent activation of cell cycle checkpoints.

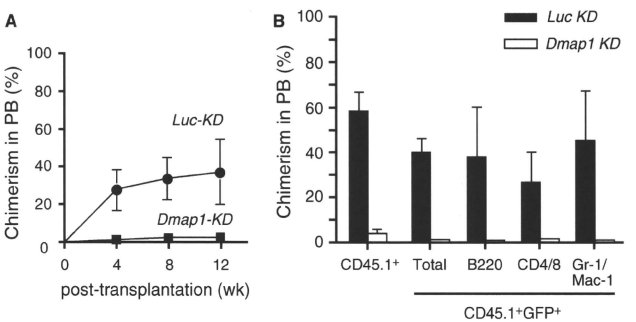

Fig. 3 *Dmap1*-knockdown HSCs show multi-lineage differentiation, but their repopulating capacity in vivo is impaired. *Luc*-KD or *Dmap1*-KD HSCs were transplanted into lethally irradiated recipient mice (50 HSCs/mice) together with 2×10^5 BM competitor cells. **a** Percent chimerism in *Luc*-KD or *Dmap1*-KD peripheral blood cells expressing both Ly5.2 and GFP is depicted ($n = 6$). **b** Percent chimerism in each lineage is depicted ($n = 6$)

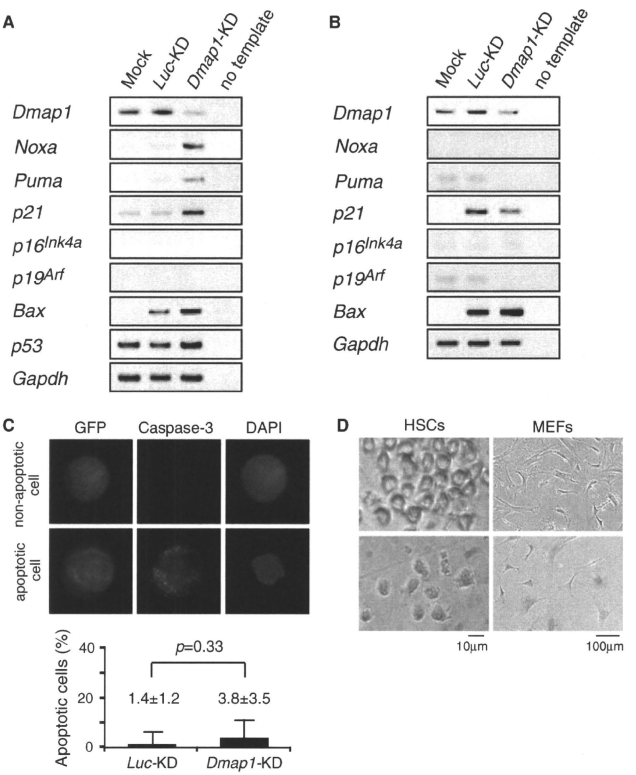

Fig. 4 Depletion of Dmap1 leads to the altered transcription of p53 target genes. **a, b** A semi-quantitative RT-PCR analysis was performed using untransduced (mock), *Luc*-KD or *Dmap1*-KD wild type (in **a**) or $p53^{-/-}$ (in **b**) $CD34^-KSL$ HSCs at 72 h after transduction. PCR was performed for 35 cycles. **c** Apoptotic assays. *Luc*-KD or *Dmap1*-KD $CD34^-KSL$ HSCs at 72 h after transduction were stained with an anti-active caspase-3 antibody to evaluate apoptosis. Photomicrographs of representative non-apoptotic and apoptotic cells are depicted in *upper panels*. GFP (*green*), active caspase-3 (*red*), and nuclear 4′,6-diamidino-2-phenylindole (DAPI) (*blue*). Percent apoptotic cells were calculated and indicated in *bar graphs* ($n = 500$). **d** Detection of SA-β-galactosidase activity. *Luc*-KD or *Dmap1*-KD $CD34^-KSL$ HSCs at 72 h after transduction (*upper panel*) were examined for SA-β-galactosidase activity (*lower panel*). *Dmap1*-KD MEFs were used as a positive control

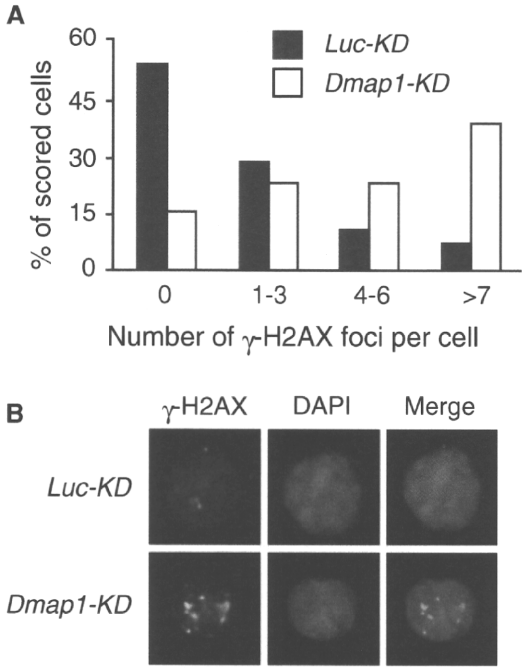

Fig. 5 *Dmap1*-knockdown causes DNA breaks. **a** Number of γ-H2AX foci expressed per cell in *Luc*-KD or *Dmap1*-KD HSCs. At 72 h after transduction, HSCs were subjected to immunofluorescent staining for γ-H2AX. The results are shown as means for two independent experiments. **b** Representative images of γ-H2AX immunostaining in *Luc*-KD or *Dmap1*-KD CD34$^-$KSL cells

Unexpectedly, *Dmap1*-knockdown in *p53*$^{-/-}$ HSCs still suppressed the proliferative capacity of HSCs in vitro (Fig. 6a) and the percentage of GFP$^+$-infected cells progressively decreased in the *Dmap1*-knockdown culture, while it remained at a high level in the control *Luciferase*-knockdown culture (Fig. 6b). *Dmap1*-knockdown *p53*$^{-/-}$ HSCs still showed an impaired capacity to repopulate for both short and long term (Fig. 6c), suggesting that *p53*-deficiency was not sufficient to restore the impaired self-renewal capacity of *Dmap1*-depleted HSCs.

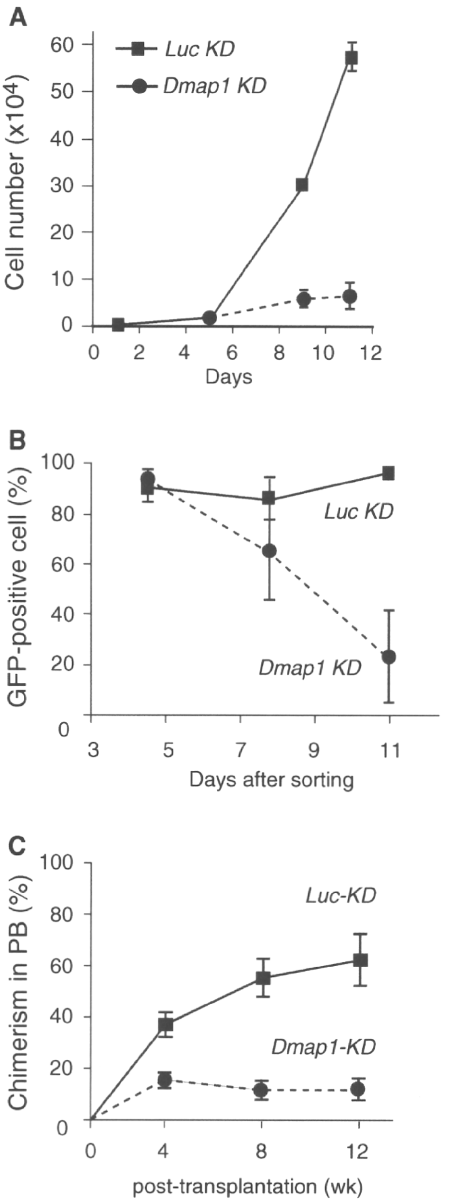

Fig. 6 Dmap1-depleted HSCs show severely impaired proliferation and self-renewal even in a *p53*-deficient background. **a** Growth curve of *Luc*-KD or *Dmap1*-KD CD34$^-$KSL *p53*$^{-/-}$ HSCs in vitro. **b** Percentage of GFP-positive cells among *Luc*-KD or *Dmap1*-KD CD34$^-$KSL *p53*$^{-/-}$ HSCs in vitro. GFP-positive cells in *Luc*-KD or *Dmap1*-KD *p53*$^{-/-}$ HSC cultures were determined by flow cytometric analysis on the indicated days. The results are shown as the mean ± SD for triplicate cultures. **c** Contribution of *Dmap1*-KD HSCs to hematopoiesis. *Luc*-KD or *Dmap1*-KD *p53*$^{-/-}$ HSCs were transplanted into lethally irradiated recipient mice (50 HSCs/mice) together with 2×10^5 BM competitor cells. Percent chimerism in *Luc*-KD or *Dmap1*-KD peripheral blood cells expressing both Ly5.2 and GFP at the indicated time points after BM transplantation is depicted

4 Discussion

In the present study, we showed that Dmap1, a component of the NuA4/Tip60 complex, was essential for the proliferative capacity of HSCs, but dispensable for multi-lineage differentiation both in vitro and in vivo. Depletion of Dmap1 in HSCs caused DNA damage, as evident by the formation of foci of γ-H2AX, and triggered DNA damage response (DDR) such as the activation of p53-dependent cell cycle checkpoints. These findings clearly show that depletion of Dmap1 compromises the repair process and correlate well with our previous observation in MEFs [14]. Thus, impaired HSC functions caused by *Dmap1*-knockdown could be attributed to defective DNA repair process and genomic instability. Corresponding to these findings, the NuA4/Tip60 complex has been implicated in DNA repair. Expression of a Tip60 mutant and *Trrap*-

knockdown has been reported to impair homologous recombination repair. In *Trrap*-deficient cells, the loading of repair proteins is impaired at sites of DNA damage because of impeded relaxation of the chromatin [22]. In contrast, we demonstrated that *Dmap1*-knockdown in MEFs did not compromise the loading of repair proteins, but inhibited accumulation of PCNA at the damaged sites [14], suggesting that Dmap1 functions at the later phase of DNA repair than Trrap does.

DNA damage is intimately linked to stem cell aging. Heritable DNA damage accrued in stem cells leads to stem cell senescence or apoptosis, which over time could lead to depletion of the stem cell pool and reduced regenerative capacity of stem cells, the physiological hallmarks of aging [15]. The crucial role of the DNA repair machinery for the maintenance of HSCs has been demonstrated in analyses of mice deficient in factors involved in nucleotide excision repair, non-homologous end joining and telomere maintenance [16, 17]. Eukaryotic cells frequently encounter environmental stress, such as ionizing radiation or chemical exposure, or endogenously programmed events, such as V(D)J recombination and the stalling of DNA replication forks, which can generate DNA strand breaks and provoke the activation of cell cycle checkpoints [23]. To maintain genomic integrity, cells have evolved a number of pathways that recognize, respond to and repair different forms of damaged DNA. Our findings indicate that Dmap1 is one of those molecules conserved from yeast to humans.

The cell cycle checkpoints function as a genome surveillance mechanism to regulate responses to DNA damage and perturbations of DNA replication. Our data demonstrated that *Dmap1*-knockdown led to DNA damage and activated p53-dependent damage-induced checkpoints. Although *Dmap1*-knockdown in $p53^{-/-}$ HSCs largely abrogated the transcriptional up-regulation of p53 target genes, *Dmap1*-depleted HSCs with a *p53*-null background still exhibited apparent defects in proliferation in vitro and long-term repopulating capacity in vivo. These findings suggest that *Dmap1*-knockdown compromises HSC functions in multiple ways, including those which are p53-independent. In ES cells, the NuA4/Tip60 complex keeps a large group of developmental genes repressed through collaboration with Nanog and polycomb-group proteins [24]. In addition, we identified that Bmi1 incorporates Dmap1 in polycomb gene silencing at least at some Bmi1 target loci [13]. Thus, it is possible that *Dmap1*-knockdown could disrupt the coordinated gene silencing by the NuA4/Tip60 complex and the PcG complexes in HSCs, leading to de-repressed expression of developmental genes in HSCs. It would be intriguing to further examine how the NuA4/Tip60 complex collaborates with the PcG complexes in the context of regulation of HSC identity.

Acknowledgments We thank Dr. Hiroyuki Miyoshi, RIKEN Bioresource Center for the CS-H1-shRNA-EF-1α-EGFP vector. This work was supported in part by Grants-in-Aid for Scientific Research (#20052009) and the Global COE Program (Global Center for Education and Research in Immune System Regulation and Treatment), MEXT, Japan, a Grant-in-aid for Core Research for Evolutional Science and Technology (CREST) from the Japan Science and Technology Corporation (JST) and a grant from the Takeda Science Foundation.

References

1. Surani MA, Hayashi K, Hajkova P. Genetic and epigenetic regulators of pluripotency. Cell. 2007;128:747–62.
2. Morrison AJ, Shen X. Chromatin remodelling beyond transcription: the INO80 and SWR1 complexes. Nat Rev Mol Cell Biol. 2009;10:373–84.
3. Kouzarides T. Chromatin modifications and their function. Cell. 2007;128:693–705.
4. Rountree MR, Bachmann KE, Baylin SB. DNMT1 binds HDAC2 and a new co-repressor, DMAP1, to form a complex at replication foci. Nat Genet. 2000;25:269–77.
5. Cai Y, Jin J, Tomomori-Sato C, et al. Identification of new subunits of the multiprotein mammalian TRRAP/TIP60-containing histone acetyltransferase complex. J Biol Chem. 2003;278:42733–6.
6. Conaway RC, Conaway JW. The INO80 chromatin remodeling complex in transcription, replication and repair. Trends Biochem Sci. 2009;34:71–7.
7. Boyer LA, Latek RR, Peterson CL. The SANT domain: a unique histone-tail-binding module? Nat Rev Mol Cell Biol. 2004; 5:158–63.
8. Peterson CL, Côté J. Cellular machineries for chromosomal DNA repair. Genes Dev. 2004;18:602–16.
9. Auger A, Galarneau L, Altaf M, et al. Eaf1 is the platform for NuA4 molecular assembly that evolutionarily links chromatin acetylation to ATP-dependent exchange of histone H2A variants. Mol Cell Boil. 2008;28:2257–70.
10. Molofsky AV, Pardal R, Iwashita T, Park IK, Clarke MF, Morrison SJ. Bmi-1 dependence distinguishes neural stem cell self-renewal from progenitor proliferation. Nature. 2003;425:962–7.
11. Park IK, Qian D, Kiel M, et al. Bmi-1 is required for maintenance of adult self-renewing haematopoietic stem cells. Nature. 2003;423:302–5.
12. Iwama A, Oguro H, Masamitsu N, et al. Enhanced self-renewal of hematopoietic stem cells mediated by the polycomb gene product Bmi-1. Immunity. 2004;21:843–51.
13. Negishi M, Saraya A, Miyagi S, et al. Bmi1 cooperates with Dnmt1-associated protein 1 in gene silencing. Biochem Biophys Res Commun. 2007;353:992–8.
14. Negishi M, Chiba T, Saraya A, Miyagi S, Iwama A. DMAP1 is essential for the recruitment of PCNA to repair foci. Genes Cells. 2009;14:1347–57.
15. Rossi DJ, Jamieson CH, Weissman IL. Stems cells and the pathways to aging and cancer. Cell. 2008;132:681–96.
16. Rossi DJ, Seita J, Czechowicz A, Bhattacharya D, Bryder D, Weissman IL. Hematopoietic stem cell quiescence attenuates DNA damage response and permits DNA damage accumulation during aging. Cell Cycle. 2007;6:2371–6.
17. Nijnik A, Woodbine L, Marchetti C, et al. DNA repair is limiting for haematopoietic stem cells during ageing. Nature. 2007; 449:288–91.
18. Osawa M, Hanada K, Hamada H, Nakauchi H. Long-term lymphohematopoietic reconstitution by a single CD34-low/negative hematopoietic stem cell. Science. 1996;273:242–5.

19. Sapountzi V, Logan IR, Robson CN. Cellular functions of TIP60. Int J Biochem Cell Biol. 2006;38:1496–509.
20. Löbrich M, Jeggo PA. The impact of a negligent G2/M checkpoint on genomic instability and cancer induction. Nat Rev Cancer. 2007;7:861–9.
21. Srivastava N, Gochhait S, De Boer P, Bamezai RN. Role of H2AX in DNA damage response and human cancers. Mutat Res. 2009;681:180–8.
22. Murr R, Loizou JI, Yang YG, et al. Histone acetylation by Trrap-Tip60 modulates loading of repair proteins and repair of DNA double-strand breaks. Nat Cell Biol. 2006;8:91–9.
23. Khanna KK, Jackson SP. DNA double-strand breaks: signaling, repair and the cancer connection. Nat Genet. 2001;27:247–54.
24. Fazzio TG, Huff JT, Panning B. An RNAi screen of chromatin proteins identifies Tip60-p400 as a regulator of embryonic stem cell identity. Cell. 2008;134:162–74.

Journal of Plastic, Reconstructive & Aesthetic Surgery (2010) 63, 1990–1994

JPRAS
An International Journal of Surgical Reconstruction
www.JPRASurg.com

Midfacial distraction using a transfacial pinning technique for syndromic craniosynostosis with obstructive respiratory disorders

Nobuyuki Mitsukawa [a,*], **Kaneshige Satoh** [b]

[a] *Department of Plastic and Reconstructive Surgery, Showa University, Faculty of Medicine, 1-5-8, Hatanodai, Shinagawa-ku, Tokyo 142-8666, Japan*
[b] *Department of Plastic and Reconstructive Surgery, Chiba University, Faculty of Medicine, Chiba, Japan*

Received 5 November 2009; accepted 22 January 2010

KEYWORDS
Midfacial distraction osteogenesis;
Transfacial pinning technique;
Syndromic craniosynostosis;
Obstructive sleep apnoea

Summary Syndromic craniosynostosis is known to be associated with various obstructive respiratory disorders including sleep apnoea. We performed early midfacial distraction using a transfacial pinning technique in five syndromic craniosynostotic patients with obstructive respiratory disorders. Here, we report good results, indications and usefulness of this procedure. The subjects were five young children aged 7 months to 2 years who had respiratory disorders since birth due to midface hypoplasia. All subjects underwent midfacial distraction to avoid tracheotomy. The method involved Le Fort III osteotomy followed by the use of our original transfacial pinning system. This system consisted of devices connecting (1) transfacial pins penetrating the bilateral zygomatic bones and (2) Kirschner wires, which were passed through plates fixed on the bilateral temporal bones. The maxilla was distracted anteriorly at least 20 mm. Distraction was evaluated by comparing the pre- and postoperative polysomnography (PSG) and cephalograms. All patients had markedly improved respiratory conditions after distraction, and a tracheotomy was avoided. Postoperative PSG and cephalograms also showed great improvements compared with preoperative findings. A transfacial pinning system was considered useful and can be the most suitable method for early midfacial distraction in syndromic craniosynostosis with obstructive respiratory disorders.
Published by Elsevier Ltd on behalf of British Association of Plastic, Reconstructive and Aesthetic Surgeons.

There has been much attention focussed on obstructive sleep apnoea (OSA) as one of the causes of sudden death in patients with syndromic craniosynostosis with midface hypoplasia. In this study, we performed early midfacial distraction using a transfacial pinning technique in young children with syndromic craniosynostotic and severe obstructive respiratory disorders. We achieved relatively good results using this procedure.

* Corresponding author. Tel.: +81 3 3784 8548; fax: +81 3 3784 9183.
E-mail address: nmitsu@air.linkclub.or.jp (N. Mitsukawa).

1748-6815/$ - see front matter Published by Elsevier Ltd on behalf of British Association of Plastic, Reconstructive and Aesthetic Surgeons.
doi:10.1016/j.bjps.2010.01.029

Methods and materials

The subjects were five young children (two boys and three girls) aged 7 months to 2 years 8 months (mean age: 18.4 months). These children had obstructive respiratory disorders such as sleep apnoea and severe snoring since birth due to midface hypoplasia. There were three children with Crouzon syndrome and two children with Pfeiffer syndrome (Table 1). The method involved polysomnography (PSG) to confirm that the cause of the respiratory disorder was peripheral due to midface hypoplasia. Enlargement of the upper airway was planned using midfacial distraction to avoid tracheotomy.

The surgery involved Le Fort III osteotomy followed by the use of our original transfacial pinning system (Medical U&A Inc., Osaka, Japan). This system consisted of devices connecting (1) transfacial pins penetrating the bilateral zygomatic bones and (2) Kirschner wires, which were passed through plates fixed on the bilateral temporal bones (Figure 1). The midface was distracted anteriorly using this system. The Kirschner wire in the temporal region was bent in a 'U' shape. Only the plate was used for fixation without penetration through the temporal bone. This method allowed for more mobility and flexibility, and it accommodated the wound to a certain extent. A transfacial pin with a diameter of 2.0 mm or more was used to avoid flexure of the pin as much as possible during distraction. Pins were inserted so that they penetrated the bilateral zygomatic bones. Young children with syndromic craniosynostosis have small zygomatic bones and maxillae and high arched palates. Thus, the insertion of a pin is not easy requiring adequate precaution. Distraction was initiated a few days after surgery and performed with consideration for respiratory conditions, facial morphology and occlusal conditions. All subjects had at least 20 mm of distraction. In three of five subjects, front-orbital distraction using an internal device was performed simultaneously for intracranial hypertension and cranial deformation. Transfacial pins were removed approximately 2–3 months after the completion of distraction. Changes in the maxillary area and percentages of enlargement were measured using cephalograms taken during a 1-year period after the removal of the transfacial pin (Figure 2). In addition, improvements were evaluated by PSG.

Results

Slight flexure of pins was observed in two cases during distraction, but their progress was uneventful; a portion of the pin that penetrated the bilateral zygomatic bones was exposed in the palatal area in one case. Presently, 2 years to 4 years 6 months have passed since surgery, and 1-year 9 months to 4 years 3 months have passed since the removal of the transfacial pin. In all cases, the frequency of OSA was markedly reduced after surgery, respiratory conditions were greatly improved and tracheotomy was avoided. All subjects had maxillary enlargement in postoperative cephalograms, and analysis of PSG also showed great improvement. In all subjects, there was a scar of a few millimetres in bilateral cheeks where transfacial pins were inserted, but there were no major complications associated with distraction (Tables 2 and 3).

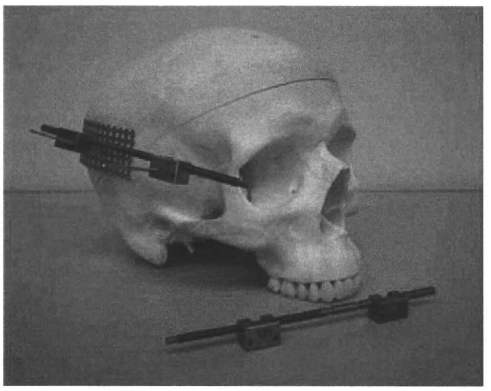

Figure 1 Transfacial pinning system (Medical U&A Inc., Japan).

Case reports

Case 2

The patient was an 8-month-old boy with Pfeiffer syndrome. He had a severe respiratory disorder and OSA since birth and required airway management during sleep. Thus, long-term hospitalisation was unavoidable (Figure 3(A)–(C)). Front-orbital advancement and ventriculo-peritoneal (V-P) shunt surgery were performed 2 months and 5 months after birth, respectively. In this study, midfacial distraction using a transfacial pinning technique was performed to avoid tracheotomy. Distraction was initiated a few days after surgery and left and right sides were distracted a total of 21.7 mm per side at a rate of 1.4 mm per day (Figure 3(D)). The frequencies of snoring and OSA decreased markedly after surgery, and respiratory

Table 1 Cases

Case No.	Age	Diagnosis (syndrome)	Distraction method	Distraction distance (mm)	Follow-up (mo)
1	7 months	Pfeiffer	*Le Fort III + FOD	21	54
2	8 months	Pfeiffer	*Le Fort III	21.7	24
3	1 year	Crouzon	*Le Fort III + FOD	22.4	33
4	2 years	Crouzon	*Le Fort III + FOD	25.9	36
5	2 years	Crouzon	*Le Fort III	25.9	28

* Le Fort III: Transfacial pinning method.
* FOD: Front-orbital distraction.

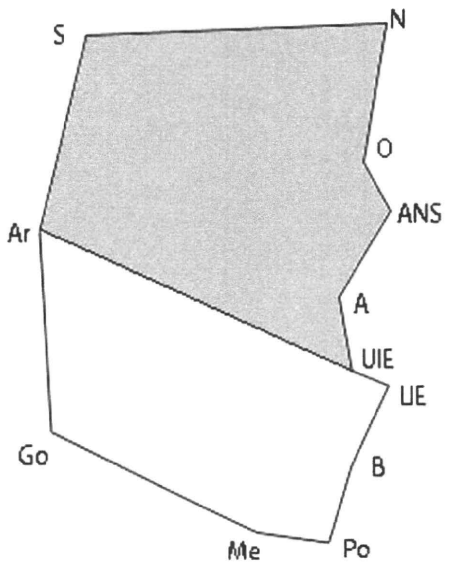

Figure 2 The area of upper face (shaded area). S: Sella turcica, N: Nasion, O: Orbitale, ANS: Anterior nasal spine, A: Point A, UIE: Upper incisal edge, Ar: Articulare.

conditions were greatly improved (Figure 3(E) and (F)). The analysis of pre- and postoperative cephalograms revealed that the area of the maxilla had increased from 15.8 to 24.6 cm^2, and enlargement of the upper airway space was confirmed (Figure 3(G)). PSG showed marked improvement in the apnoea–hypopnea index (AHI) which was 23.6 preoperatively and 2.6 one year postoperatively (9 months after pin removal).

Case 4

The patient was a 2-year-old girl with Crouzon syndrome. She had repeated severe snoring and OSA since birth due to midface hypoplasia and required airway management during sleep (Figure 4(A)–(C)). Thus, she was hospitalised long-term. She underwent monobloc distraction using an internal device at the age of 1 year. However, the results were unsatisfactory because of a fracture along the maxillozygomatic suture. In this study, front-orbital distraction using an internal device was performed simultaneously with midfacial distraction using a transfacial pinning technique. Distraction was performed a total of 25.9 mm on each side at a rate of 1.4 mm per day relative to the midface (Figure 3(D) and (E)). Postoperatively, the respiratory conditions improved markedly, OSA was resolved, and the patient was discharged from the hospital (Figure 3(F) and (G)). The analysis of pre- and postoperative cephalograms revealed that the area of the maxilla had increased from 23.2 to 41.6 cm^2, and enlargement of the upper airway space was confirmed (Figure 3(H)). PSG showed marked improvement in AHI, which was 19.2 preoperatively and 1.6 1 year and 6 months postoperatively (1 year 3 months after pin removal).

Discussion

Indications for the treatment of syndromic craniosynostosis, such as Crouzon syndrome and Apert syndrome, include intracranial hypertension, severe exophthalmos, obstructive respiratory disorder, occlusal disharmony and cranial facial deformations. Treatment of a respiratory disorder must be an urgent and major objective just as for intracranial hypertension and severe exophthalmos. Upper airway stenosis can occur in syndromic craniosynostosis due to midface hypoplasia. Therefore, a tracheotomy is performed in severe cases. In recent years, based on our past reflectable experience[1] that a patient with Crouzon syndrome died suddenly due to OSA during the waiting period of midfacial distraction, we have been performing early midfacial distraction in young children to avoid tracheotomy. In general, Le Fort III midfacial distraction and monobloc distraction are accepted as standard surgical techniques for syndromic craniosynostosis with obstructive respiratory disorders.[2–5] Flores et al.[6] examined the clinical courses and analysed the cephalograms of 20 patients, who underwent Le Fort III distraction. They found that nasopharyngeal and velopharyngeal airspaces had enlarged and respiratory conditions improved after Le Fort III distraction. Nine of 10 patients with significant airway compromise experienced improvement in their symptoms of OSA or had their tracheotomy removed.

There are external and internal types of device for midfacial distraction. It is difficult to appropriately differentiate their uses, and selection of device type is often a challenge. The crania of young children are thin and brittle, and therefore, it is difficult to use a typical external device – a halo-type external distraction device.[7] In addition, one must be cautious of intracranial injuries from falls.[8] For an internal type distraction device, it is difficult to distract while maintaining parallelism of left and right sides. Vulnerability of the maxillozygomatic suture is particularly concerning for cases with severe temporal

Table 2 Results (1)–Analyzing the measurement on cephalogram.

Case No.	The area of upper face		Rate of increase (%)
	Pre-distraction (cm^2)	Post-distraction (cm^2)	
1	14.2	21.5	51.4
2	15.8	24.6	43.0
3	19.2	29.2	52.1
4	23.2	41.6	79.3
5	24.1	35.8	48.5

Table 3 Results (2)—Analyzing polysomnography (PSG).

Case No.	Mean blood oxygen saturation (%)		Apnoea–hypopnea index (AHI) (times/h)	
	Pre-distraction (cm^2)	Post-distraction (cm^2)	Pre-distraction (cm^2)	Post-distraction (cm^2)
1	91	98	18.8	1.7
2	89	98	23.6	2.6
3	95	99	14.1	0.8
4	92	98	19.2	1.6
5	94	99	17.7	0.8

bulging. We have reported two cases of maxillozygomatic fracture during midfacial distraction using an internal device in syndromic craniosynostosis.[9]

In this study, we examined five young children with syndromic craniosynostosis and severe obstructive respiratory disorders. We performed midfacial distraction using a transfacial pinning technique and obtained relatively good results. The only previous reports on transfacial pinning techniques were by Arnaud et al.[10] and Pellerin et al.[11] There has been no comprehensive report clearly describing its indications and usefulness. The transfacial pinning system is an external device. It has fewer risks such as for intracranial injuries and is safer than the halo type. In addition, this system is less cumbersome to wear than the halo type. In this system, one can expect certainty of results similar to a halo type. Unlike an internal device, there is no concern for fracture along the maxillozygomatic suture because this system advances the maxilla *en bloc*. In this study, we performed morphological evaluation by analysing the maxillary areas from lateral cephalograms. We performed functional evaluation by PSG analysis. Improvements were observed in both evaluations. Thus, midfacial distraction using a transfacial pinning technique was demonstrated to be a very effective procedure for avoiding tracheotomy in syndromic cranosynostotic patients with obstructive respiratory disorders. It has been 2 years to 4 years 6 months after surgery, and the progress of the five subjects has been favourable. There has not been any recurrence of obstructive respiratory disorders including OSA. However, these subjects are patients who might have latent development of maxillary hypoplasia. Thus, it is necessary to carefully follow-up with consideration for future growth.

A transfacial pinning technique can be the most suitable method for early midfacial distraction in syndromic

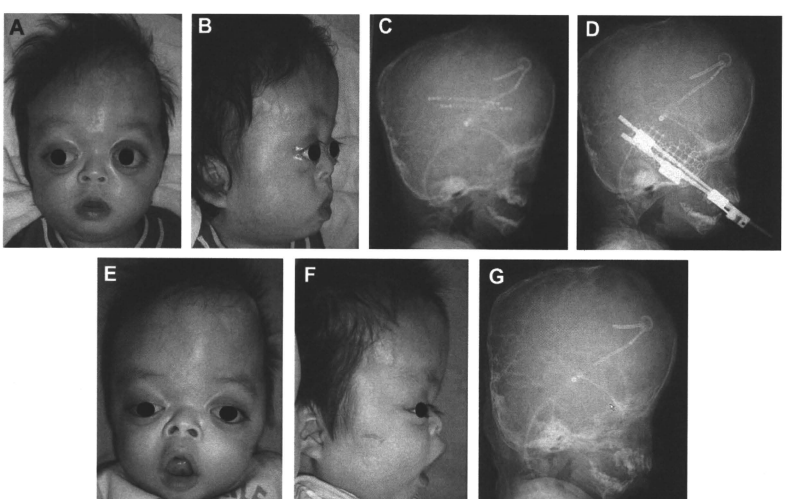

Figure 3 Case 2: Preoperative frontal (A) and lateral (B) views, and lateral cephalogram (C), of a 8-month-old male infant with Pfeiffer syndrome, and severe apnea episodes, (D) Lateral cephalogram of patient with transfacial pinning system in place during consolidation period. Postoperative frontal (E) and lateral (F) views, and lateral cephalogram (G) at 12 months of age.

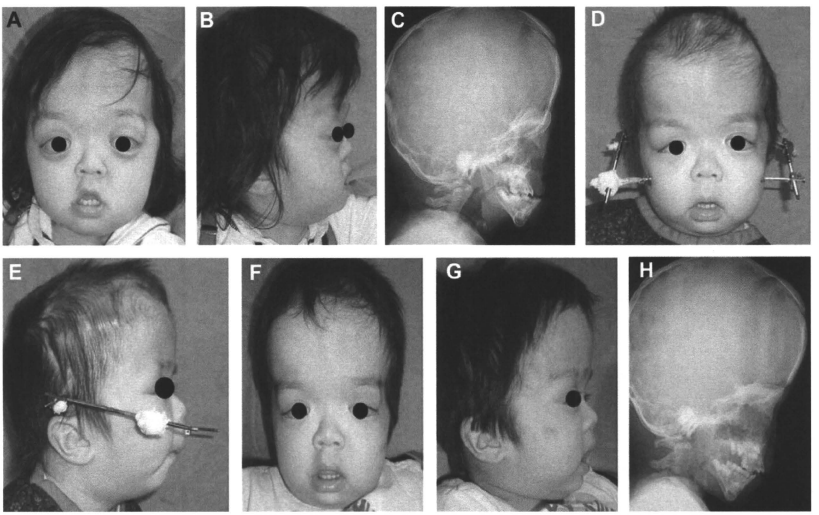

Figure 4 Case 4: Preoperative frontal (A) and lateral (B) views, and lateral cephalogram (C), of a 2-year-old female infant with Crouzon syndrome, and severe apnea episodes. Postoperative frontal (D) and lateral (E) views of patient with transfacial pinning system in place during consolidation period. Postoperative frontal (F) and lateral (G) views, and lateral cephalogram (H) at 18 months of age.

craniosynostotic young children with obstructive respiratory disorders.

Disclosure

The authors have no any financial interests and personal relationships with other people or organisations to declare.

Acknowledgement

We greatly appreciate Professor Philipe Pellerin's courtesy and kindness in fabricating an apparatus of the transfacial pinning system.

References

1. Mitsukawa N, Satoh K, Hayashi T, et al. A reflectable case of obstructive sleep apnea in an infant of Crouzon syndrome. *J Craniofac Surg* 2004;**15**:874–8.
2. Mathijssen I, Arnaud E, Marchac D, et al. Respiratory outcome of midface advancement with distraction: a comparison between Le Fort III and frontofacial monobloc. *J Craniofac Surg* 2006;**17**:642–4.
3. Arnaud E, Marchac D, Renier D. Reduction of morbidity of the frontofacial monobloc advancement in children by the use of internal distraction. *Plast Reconstr Surg* 2007;**120**:1009–26.
4. Fearon JA. Halo distraction of the Le Fort III in syndromic craniosynostosis: a long-term assessment. *Plast Reconstr Surg* 2005;**115**:1524–36.
5. Shetye PR, Boutros S, Grayson BH, et al. Midterm follow-up of midface distraction for syndromic craniosynostosis: a clinical and cephalometric study. *Plast Reconstr Surg* 2007;**120**: 1621–32.
6. Flores RL, Shetye PR, Zeitler D, et al. Airway changes following Le Fort III distraction osteogenesis for syndromic craniosynostosis: a clinical and cephalometric study. *Plast Reconstr Surg* 2009;**124**:590–601.
7. Le BT, Eyre JM, Wehby MC, et al. Intracranial migration of halo fixation pins: a complication of using an external distraction device. *Cleft Palate-Craniofac J* 2001;**38**:401–4.
8. Rieger J, Jackson IT, Topf JS, et al. Traumatic cranial injury sustained from a fall on the rigid external distraction device. *J Craniofac Surg* 2001;**12**:237–41.
9. Mitsukawa N, Satoh K, Hayashi T, et al. Salvaged Le Fort II halo distraction for an unfavorable outcome of midfacial distraction using an internal device in syndromic craniosynostosis. *Plast Reconstr Surg* 2004;**113**:1219–24.
10. Arnaud E, Marchac D, Renier D. Distraction osteogenesis with double internal devices combined with early frontal facial advancement for the correction of facial craniosynostosis: report of clinical cases. *Ann Chir Plast Esthet* 2001;**46**:268–76.
11. Pellerin P, Capon-Desgardin N, Martinot-Duquennoy V, et al. Mid-facial distraction without osteotomy with a trans-facial pin: report of 4 clinical cases. *Ann Chir Plast Esthet* 2001;**46**: 277–84.

Journal of Plastic, Reconstructive & Aesthetic Surgery (2010) 63, e611–e614

ELSEVIER

JPRAS
An International Journal of Surgical Reconstruction
www.JPRASurg.com

CASE REPORT

Maxillomandibular distraction osteogenesis for Marshall–Smith syndrome

Nobuyuki Mitsukawa [a,*], **Kaneshige Satoh** [b]

[a] *Department of Plastic and Reconstructive Surgery, Showa University, Faculty of Medicine, 1-5-8, Hatanodai, Shinagawa-ku, Tokyo 142-8666, Japan*
[b] *Department of Plastic and Reconstructive Surgery, Chiba University, Faculty of Medicine, Chiba, Japan*

Received 6 November 2009; accepted 22 January 2010

KEYWORDS
Marshall–Smith syndrome;
Maxillomandibular distraction;
Craniofacial anomalies

Summary The Marshall–Smith syndrome is a very rare disorder with early overgrowth and was first reported by Marshall et al. in 1971. Patients with the Marshall–Smith syndrome have characteristic facial features and systemic congenital abnormalities. In many cases, patients die early in the postnatal period due to respiratory disorders. We treated a male child with this syndrome with plastic surgery to improve facial features – the first effort of its kind in the world. We report good results from the surgery. The treatment included bilateral mandibular distraction osteogenesis for micrognathia and tracheostomy weaning. Six months later, LeFort III maxillary distraction osteogenesis was performed for maxillary hypoplasia. The clinical course was uneventful after both surgeries. At the time of this report, facial appearance and occlusal conditions have improved markedly, although the tracheal stoma could not be closed. The patient is a long-term survivor of this condition. After considering quality-of-life issues for the patient, surgical treatment was offered for facial dysmorphism. This type of effort has not yet been reported in the literature. For patients with the Marshall–Smith syndrome who are expected to survive long, surgical treatment should be strongly considered to improve the quality of life of the affected child.
Published by Elsevier Ltd on behalf of British Association of Plastic, Reconstructive and Aesthetic Surgeons.

Patients with Marshall–Smith syndrome have characteristic facial features and systemic congenital abnormalities. It is a very rare disorder. This report describes a 4-year-old child with Marshall–Smith syndrome whom we treated with maxillomandibular distraction osteogenesis to improve his facial appearance. We report good results from surgical intervention. This effort is the first of its kind reported in the world literature.

* Corresponding author. Tel.: +81 3 3784 8548; fax: +81 3 3784 9183.
E-mail address: nmitsu@air.linkclub.or.jp (N. Mitsukawa).

1748-6815/$ - see front matter Published by Elsevier Ltd on behalf of British Association of Plastic, Reconstructive and Aesthetic Surgeons.
doi:10.1016/j.bjps.2010.01.028

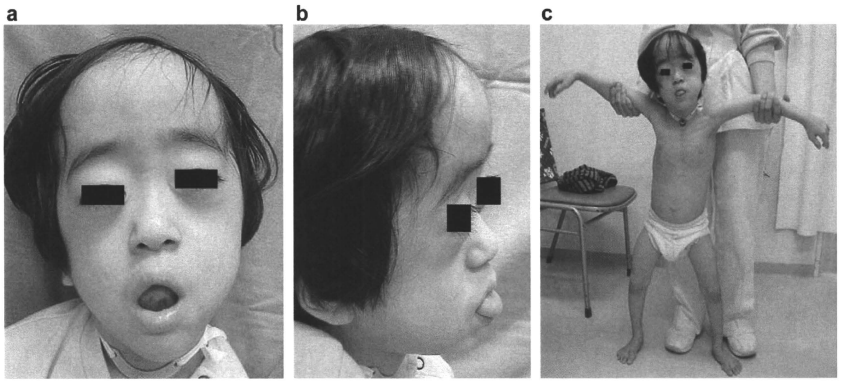

Figure 1 Preoperative findings: (a) frontal view of the face (b) lateral view of the face and (c) whole body view.

Case report

The patient was a male child who was born by vaginal delivery and weighed 2930 g after 39 weeks of gestation. He had severe respiratory distress since birth and underwent a tracheostomy 1 week after birth. When the patient was 1 year old, he was diagnosed with the Marshall–Smith syndrome from his physical appearance by a paediatrician. In October 2004, he was referred to our department for treatment of facial dysmorphism. The following features characteristics of the Marshall–Smith syndrome were found in our patient (Figure 1(a)–(c)). At the initial examination in our department, distinct facial features associated with the Marshall–Smith syndrome were noted: a prominent forehead, relative exophthalmos with shallow orbits, blue sclera, a flat nose, midface retrusion from maxillary hypoplasia, micrognathia from mandibular ramus hypoplasia and an enlarged tongue. The thorax had a short width relative to length and the trunk was long and narrow. The following radiographic findings were also seen: thin and long ribs, thoracolumbar scoliosis, wide barrel-shaped metacarpals, small distal phalanges, narrow and long diaphyses and leg bones with epiphyseal regions flaring like a fan. Craniofacial three-dimensional computed tomography (3D CT) showed that the anterior fontanel had already closed. There was a prominent forehead (dolichocephaly), large antero-posterior cranial length and a scaphocephalic state. The bilateral orbits were shallow, large in their outlines and wide in the transverse and vertical planes. There was also protrusion of the eyes (Figure 2). No abnormal findings in the brain were observed; however, his intelligence quotient (IQ) was 42, indicating mental retardation. The patient had decreased muscle tone but was able to walk. The patient was predicted to have a moderate life expectancy and his family strongly desired treatment of the facial dysmorphism. Thus, surgical treatment was performed after consideration of the aforementioned points.

First, micrognathia was treated by bilateral mandibular distraction osteogenesis, which was also performed for

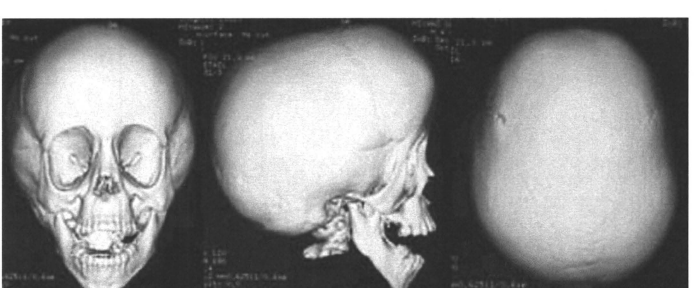

Figure 2 Craniofacial 3D CT image.

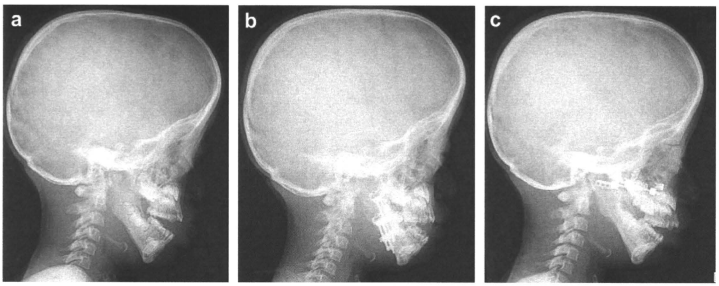

Figure 3 Cephalograms (lateral view). (a) Preoperative (b) after mandibular distraction osteogenesis (c) after maxillary distraction osteogenesis.

tracheostomy weaning. Mandibular angle osteotomy was performed and distraction of a total of 15 mm was achieved using an internal device. Ensuring the direction of mandibular distraction to be parallel to the occlusal plane was technically challenging. To improve bone morphology and respiratory condition, we performed distraction in an inferior–anterior direction with a downward tendency relative to the occlusal plane. Six months later, LeFort III midfacial distraction was performed using an internal device for maxillary hypoplasia and exophthalmos to distract 20 mm (Figure 3(a)–(c)). At the time of surgery, the maxilla and mandible had bone morphology characteristic of the Marshall–Smith syndrome. However, bone thickness and hardness were normal. Thus, osteotomy was performed without a problem. The clinical course was uneventful after both surgeries. Unfortunately, the patient had large amounts of sputum and repeated bouts of bronchitis precluding closure of the tracheostomy site. Currently, at 2 years and 6 months from maxillary distraction, the patient's facial appearance (in particular, maxillary hypoplasia and exophthalmos) has improved markedly. The occlusal conditions with open bite have also improved. Previously, the patient's tongue was consistently protruding anteriorly, but it was no longer prominent due to increase of the intraoral volume (Figure 4(a)–(c)). Analysis was performed by cephalograms at various stages of the treatment process. Although some relapse was observed 2 years postoperatively, the maxillomandibular distraction accomplished enlargement of the airway space and reconstruction of the wide oral cavity (Table 1).

Discussion

Marshall–Smith syndrome is a very rare disorder with early overgrowth and was first reported by Marshall et al. in 1971.[1] Patients with the Marshall–Smith syndrome have characteristic facial features and systemic congenital abnormalities. In many cases, the patients die early in the postnatal period due to respiratory disorders such as bronchitis or laryngeal abnormality.[2] All previously

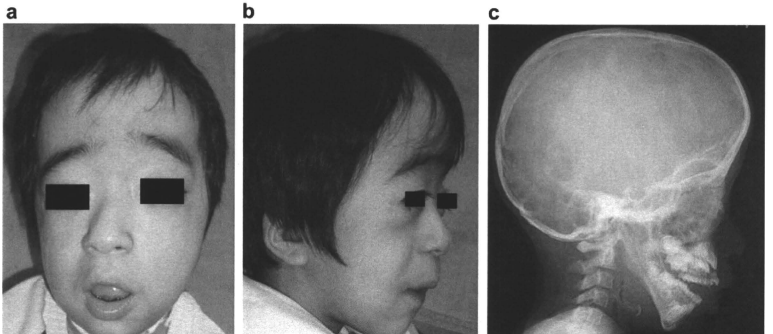

Figure 4 Two years and six months postoperatively: (a) frontal view of the face (b) lateral view of the face (c) cephalogram (lateral view).

Table 1 Analysis of pre- and postoperative cephalograms

	SNA	SNB	ANB
Preoperative	64.9°	64.7°	0.3°
Six months after mandib. distr.	65.6°	66.3°	−0.7°
Six months after maxilla. distr.	81.7°	69.4°	12.3°
Two years after maxilla. distr.	72.5°	63.5°	9.0°

reported cases of this syndrome have been sporadic without a clear genetic link or aetiology. There have been less than 40 cases of Marshall–Smith syndrome worldwide, according to our search. In Japan, there have been only five cases, including our patient.[3] Patients with the Marshall–Smith syndrome have characteristic facial features such as a prominent forehead, ocular hypertelorism, relative exophthalmos with shallow orbits, blue sclera, an upturned and flat nose, maxillary hypoplasia, hypoplasia of the mandibular ramus, an enlarged tongue and low-set ears. There have not been any previous reports on surgical treatment for abnormal craniofacial morphology in such patients. Tracheostomy was performed on our patient and his respiratory status has been stable. Long-term survival can be expected from this case and the quality of life of the patient and his family was considered. His family desired early surgery before he began to attend school. Thus, we decided on surgical treatment for facial dysmorphism of the Marshall–Smith syndrome – an effort which was unprecedented in the world literature.

Micrognathia was treated by mandibular distraction osteogenesis. Midface retrusion due to maxillary hypoplasia was treated by maxillary distraction osteogenesis. These two procedures were performed using internal devices. Although the Marshall–Smith syndrome is characterised by accelerated skeletal maturation, bone thickness and hardness were normal. Thus, osteotomy was performed without a problem. Exophthalmos and midface retrusion were corrected and a marked improvement in the facial appearance was observed. The oral volume was enlarged and protrusion of the tongue and drooling decreased as well. However, some degree of relapse was observed 2 years postoperatively and further jaw deformities are expected as the patient grows. It is possible that this patient may need re-distraction or classic orthognathic surgery in the future. Long-term follow-up for this patient is planned.

Plastic surgery – maxillomandibular distraction osteogenesis – was performed on a 4-year-old male child with the Marshall–Smith syndrome to improve his facial features. Such an effort was the first of its kind reported in the world literature and good results were obtained. If long-term survival can be expected in a patient with the Marshall–Smith syndrome, then surgical treatment should be actively considered after taking the patient's quality of life into account.

Disclosure

The authors have no any financial interests and personal relationships with other people or organisations to declare.

References

1. Marshall RE, Graham CB, Scott CR, et al. Syndrome of accelerated skeletal maturation and relative failure to thrive; a newly recognized clinical growth disorder. *J Pediatr* 1971; **78**:95–101.
2. Cullen A, Clarke TA, O'Dwyer TP. The Marshall–Smith syndrome: a review of the laryngeal complications. *Eur J Pediatr* 1997;**156**: 463–4.
3. Sumiya N, Ito Y, Hayakawa O, et al. Long-term survival of a patient with Marshall-Smith syndrome. *Scand J Plast Reconstr Surg Hand Surg* 2002;**36**:114–8.

Phosphate-activated glutaminase (GLS2), a p53-inducible regulator of glutamine metabolism and reactive oxygen species

Sawako Suzuki[a,b,1], Tomoaki Tanaka[a,b,1], Masha V. Poyurovsky[c], Hidekazu Nagano[a,b], Takafumi Mayama[a,b], Shuichi Ohkubo[d], Maria Lokshin[c], Hiroyuki Hosokawa[e], Toshinori Nakayama[e], Yutaka Suzuki[f], Sumio Sugano[f], Eiichi Sato[g], Toshitaka Nagao[g], Koutaro Yokote[a,b], Ichiro Tatsuno[a,b,2], and Carol Prives[c,2]

[a]Department of Clinical Cell Biology and [b]Division of Endocrinology and Metabolism, Chiba University Graduate School of Medicine, Chiba-shi, Chiba 260-8670, Japan; [c]Department of Biological Sciences, Columbia University, New York, NY 10027; [d]Drug Discovery and Development I, Hanno Research Institute, Taiho Pharmaceutical Co., Ltd., Hanno, Saitama 357-8527, Japan; [e]Department of Immunology, Chiba University Graduate School of Medicine, Chiba-shi, Chiba 260-8670, Japan; [f]Department of Medical Genome Sciences, Graduate School of Frontier Sciences, University of Tokyo, Kashiwa, Chiba 277-8562, Japan; and [g]Department of Anatomic Pathology, Tokyo Medical University, Shinjuku, Tokyo 160-0023, Japan

Contributed by Carol Prives, March 1, 2010 (sent for review January 6, 2010)

We identified a p53 target gene, phosphate-activated mitochondrial glutaminase (GLS2), a key enzyme in conversion of glutamine to glutamate, and thereby a regulator of glutathione (GSH) synthesis and energy production. GLS2 expression is induced in response to DNA damage or oxidative stress in a p53-dependent manner, and p53 associates with the GLS2 promoter. Elevated GLS2 facilitates glutamine metabolism and lowers intracellular reactive oxygen species (ROS) levels, resulting in an overall decrease in DNA oxidation as determined by measurement of 8-OH-dG content in both normal and stressed cells. Further, siRNA down-regulation of either GLS2 or p53 compromises the GSH-dependent antioxidant system and increases intracellular ROS levels. High ROS levels following GLS2 knockdown also coincide with stimulation of p53-induced cell death. We propose that GLS2 control of intracellular ROS levels and the apoptotic response facilitates the ability of p53 to protect cells from accumulation of genomic damage and allows cells to survive after mild and repairable genotoxic stress. Indeed, overexpression of GLS2 reduces the growth of tumor cells and colony formation. Further, compared with normal tissue, GLS2 expression is reduced in liver tumors. Thus, our results provide evidence for a unique metabolic role for p53, linking glutamine metabolism, energy, and ROS homeostasis, which may contribute to p53 tumor suppressor function.

glutathione antioxidant | glutaminolysis | tumor suppression | apoptosis

Recent evidence implicates p53 in regulation of cell metabolism, energy production, autophagy, and levels of reactive oxygen species (ROS) (1–3). In cancer cells, glucose uptake is much higher than in most normal tissues, and glycolysis persists even under aerobic conditions, a process known as the Warburg effect (4, 5). p53 plays several roles in regulating this process. For example, p53 decreases the glycolytic rate through inhibiting expression of glucose transporters (6) and phosphoglycerate mutase (7) while increasing the expression of TIGAR that reduces fructose-2,6-bisphosphate levels (8). Nevertheless, some studies report that p53 can promote at least some steps in glycolysis (9, 10). In addition, p53 has the ability to help maintain mitochondria (11, 12) and drive oxidative phosphorylation through the transcriptional activation of subunit I of cytochrome *c* oxidase (13), increased expression of cytochrome *c* oxidase (*SCO2*) (14), and induction of the ribonucleotide reductase subunit p52R2 (15).

Glutamine metabolism is another target for alteration in cancer development. Both glutamine uptake and the rate of glutaminolysis (i.e., catabolism of glutamine to generate ATP and lactate in the mitochondria) are known to increase in tumors (1, 16). In glutamine metabolism, mitochondrial glutaminase (GLS) is central in the conversion of glutamine to glutamate. Glutamate participates in regulation of mitochondrial bioenergetics in many normal and cancer cells via the tricarboxylic acid cycle for ATP production as well as antioxidant defense through GSH synthesis. The two different phosphate activated GLS isoforms GLS1 (kidney-type) and GLS2 (liver-type) in mammals are encoded by separate genes on different chromosomes (17–19). Previous data have suggested that GLS1 up-regulation is associated with increased rates of proliferation, whereas GLS2 prevalence seems to correspond with resting or quiescent cell states (17). Here we found that GLS2 is a p53-inducible gene that functions to regulate the energy supply and to protect against oxidative stress.

Results

GLS2 Is a p53 Target Gene. We used a cDNA microarray system to screen for p53-inducible genes in unstressed cells (Fig. S1*A*). Previously described and undescribed p53 targets were identified (Fig. S1*B*). Among potential new targets, phosphate activated GLS (GLS2; accession no. NM_013267) was significantly induced (approximately 7.5-fold) under these conditions (Fig. S1*B*). Consistently, GLS2 mRNA was induced in HCT116 ($p53^{+/+}$) but not ($p53^{-/-}$) cells treated with camptothecin or daunorubicin, and to approximately the same extent as was p21/CDKN1A (Fig. 1*A* and 1*B*). p53 did not induce GLS1 mRNA expression in these cells (Fig. S2). Mouse Gls2 was induced by daunorubicin in mouse embryonic fibroblasts (MEFs) expressing p53 ($p53^{+/+}$) but not in MEFs lacking p53 ($p53^{-/-}$; Fig. S3).

The human *GLS2* gene, located on chromosome 12q13, contains 18 coding exons and two possible p53 binding sites, approximately 1.4 kb (GLS2 BS1; −1,437/1,415) and 0.5 kb (GLS2 BS2; −584/−575) upstream of the first exon (Fig. 1*C*). Adenovirally transduced p53 (Adp53) bound to both BS1 and BS2 whereas endogenous p53 associated with only BS2 (Fig. 1*D*). Neither source of p53 was associated with two negative sites. These results indicate that, once activated, p53 induces expression of GLS2 mRNA by directly associating with a response element (BS2) in the *GLS2* promoter.

An anti-GLS2 antibody recognized a single polypeptide species of approximately 65 kDa, consistent with the previously reported

Author contributions: S. Suzuki, T.T., I.T., and C.P. designed research; S. Suzuki, T.T., H.N., T.M., S.O., M.L., H.H., T. Nakayama, Y.S., S. Sugano, E.S., T. Nagao, and K.Y. performed research; H.N., T.M., E.S., and T. Nagao contributed new reagents/analytic tools; T.T., M.V.P., S.O., M.L., Y.S., S. Sugano, K.Y., and C.P. analyzed data; and S. Suzuki, T.T., M.V.P., I.T., and C.P. wrote the paper.

The authors declare no conflict of interest.

See Commentary on page 7117.

[1]S. Suzuki and T. Tanaka contributed equally to this work.

[2]To whom correspondence may be addressed. E-mail: ichiro-tatsuno@faculty.chiba-u.jp or clp3@columbia.edu.

This article contains supporting information online at www.pnas.org/cgi/content/full/1002459107/DCSupplemental.